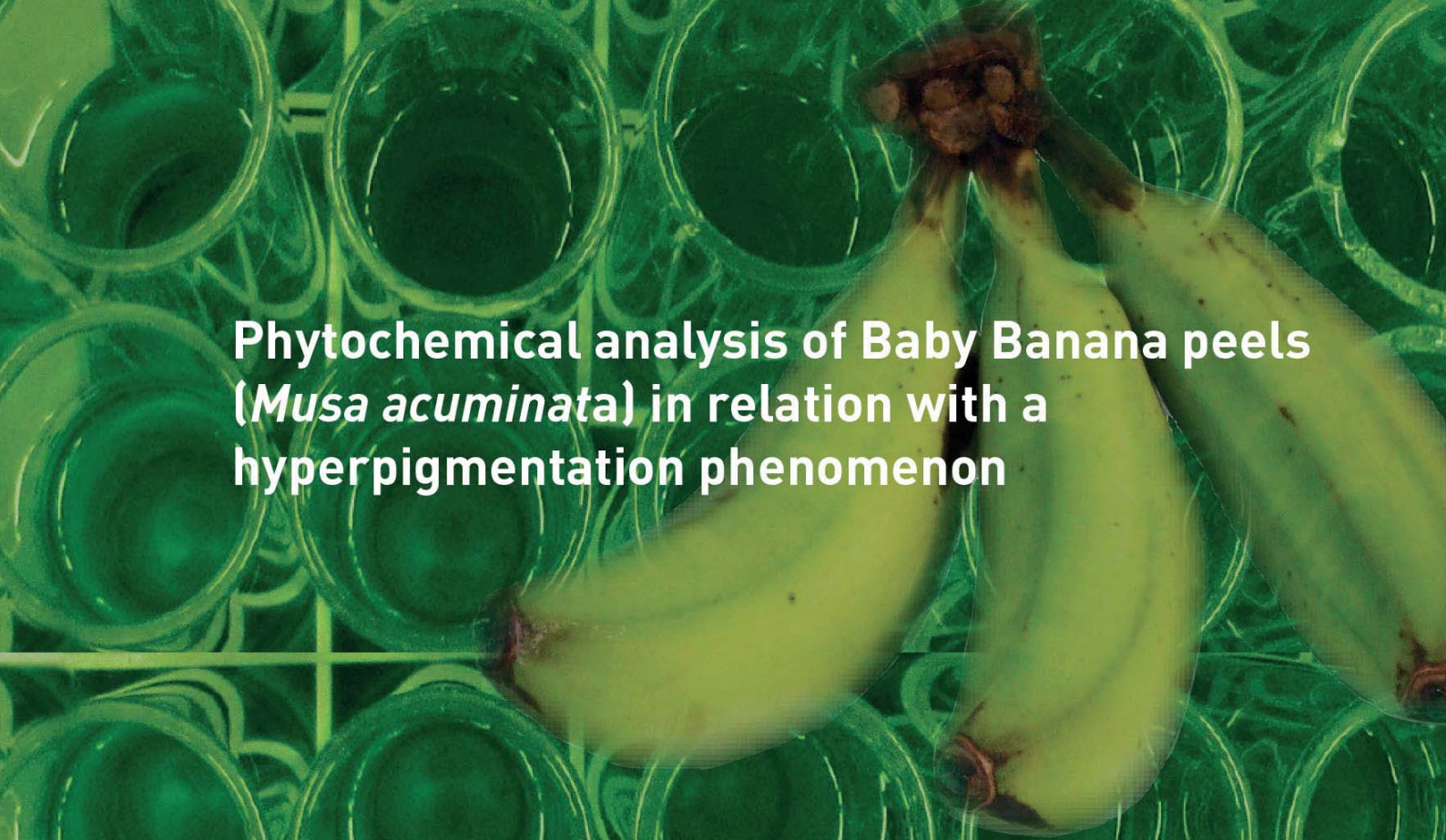

Phytochemical analysis of Baby Banana peels (*Musa acuminata*) in relation with a hyperpigmentation phenomenon

Marcela Castro-Benítez

Fakultät für Lebenswissenschaften
der Technischen Universität Carolo-Wilhelmina
zu Braunschweig

Cuvillier Verlag Göttingen
Internationaler wissenschaftlicher Fachverlag

Phytochemical analysis of Baby Banana peels (*Musa acuminata*) in relation with a hyperpigmentation phenomenon

Phytochemical analysis of Baby Banana peels (*Musa acuminata*) in relation with a hyperpigmentation phenomenon

Von der Fakultät für Lebenswissenschaften

der Technischen Universität Carolo-Wilhelmina

zu Braunschweig

zur Erlangung des Grades

einer Doktorin der Naturwissenschaften

(Dr. rer. nat.)

genehmigte

D i s s e r t a t i o n

von Marcela Elizabeth Castro Benitez
aus Bogotá /Kolumbien

Bibliografische Information der Deutschen Nationalbibliothek

Die Deutsche Nationalbibliothek verzeichnet diese Publikation in der Deutschen Nationalbibliografie; detaillierte bibliografische Daten sind im Internet über http://dnb.d-nb.de abrufbar.

1. Aufl. - Göttingen: Cuvillier, 2015

Zugl.: (TU) Braunschweig, Univ., Diss., 2015

1. Referent: Prof. Dr. Peter Winterhalter
2. Referent: apl. Professor Dr. Ulrich Engelhardt
eingereicht am: 28.01.2015
mündliche Prüfung (Disputation) am: 26.03.2015

Druckjahr 2015

Dissertation an der Technischen Universität Braunschweig,
Fakultät für Lebenswissenschaften

Nonnenstieg 8, 37075 Göttingen

Telefon: 0551-54724-0

Telefax: 0551-54724-21

www.cuvillier.de

1. Auflage, 2015

Gedruckt auf umweltfreundlichem, säurefreiem Papier aus nachhaltiger Forstwirtschaft.

ISBN 978-3-7369-9066-1

eISBN 978-3-7369-8066-2

Vorveröffentlichungen der Dissertation

Teilergebnisse aus dieser Arbeit wurden mit Genehmigung der Fakultät für Lebenswissenschaften, vertreten durch den Mentor der Arbeit, in folgenden Beiträgen vorab veröffentlicht:

Tagungsbeiträge

Castro-Benitez, M. and Winterhalter, P.: Preparative spiral coil (LSRCCC) application method for the phytochemical analysis of Baby banana peels (*Musa acuminata)* with hyperpigmentation. (Oral Presentation). XV Congreso Latinoamericano de Cromatografia y Técnicas Afines. Cartagena. Colombia. Septiembre 29th al Octubre 3rd (2014). Proceeding abstract Part 1, O-IN-04.

Castro-Benitez, M. and Winterhalter, P.: Optimization of the solvent system for the separation of chlorophylls and derivatives by means of High-Speed countercurrent chromatography in Baby banana peels, spinach and grass. (Oral Presentation) XV Congreso Latinoamericano de Cromatografia y Técnicas Afines. Cartagena. Colombia. Septiembre 29th al Octubre 3rd (2014). Proceeding abstract Part 1, O-PN-05.

Poster

Castro-Benitez, M. and Winterhalter, P.: The role of chloroform and dichloromethane as stationary phase in the solvent system for the isolation of chlorophylls and xantophylls in plants by High Speed Countercurrent Chromatography. (Poster) 8th International Conference on Countercurrent Chromatography, London, UK, July 23-25 (2014). Proceeding abstract p.195.

Castro-Benitez, M. and Winterhalter, P.: Preparative Spiral Coil-LSRCCC Application Method for the Phytochemical Analysis of Baby Banana Peels (*Musa acuminata)* with Hyperpigmentation. (Poster) 8th International Conference on Countercurrent Chromatography, London, UK, July 23-25 (2014). Proceeding abstract p.194.

Castro-Benitez, M. and Winterhalter, P.: In the search of chlorophylls in Baby banana peels and plants by means of High-Speed Countercurrent Chromatography. (Poster) 8th International Conference on Countercurrent

Chromatography, London, UK, July 23-25 (2014). Proceeding abstract p. 167.

Castro-Benitez, M., Burmeister, A., Wilde, A., Winterhalter, P.: Partial isolation of chlorophyllase enzyme and proteins in Baby banana peels (*Musa acuminata*) from Colombia. (Poster). 5. Jahrestreffen Seniorexperten Chemie. Braunschweig 6.-8. Mai (2014).

Castro-Benitez, M. and Winterhalter, P.: In the search of chlorophylls in Baby banana peels and plants by means of High-Speed Countercurrent Chromatography (Poster). Doktoranden-Kolloquium des Fachbereichs Chemie an der TU Braunschweig. (Poster). 5. Braunschweiger Jungchemiker Tagung. Braunschweig, 15. April (2014). Proceeding abstract p. 33

Castro-Benitez, M., Timpe, M., Winterhalter, P.: Isolation of Phospholipids, Glycolipids and Fatty acids from Baby Banana Peels (*Musa acuminata*) on a Preparative Scale by Means of High-Speed Countercurrent Chromatography. (Poster). Regionalverbandstagung Nord der Lebensmittelchemischen Gesellschaft. Hamburg School of Food Science, Hamburg, 24./25.3. 2014.

Castro-Benitez, M., Willeke, O., Timpe, M., Wilde, A., Winterhalter**.** P.: High Speed countercurrent chromatography for analysis of Chlorophylls *a/b* ratio and their derivates in plants. (Poster). 42. Deutscher Lebensmittelchemikertag. Braunschweig, 16.-18.9. (2013). Abstract in Kurzreferate-Band ANA 045, 151 (2013)

Castro-Benitez, M., Muñoz-Ortuño, M., Winterhalter P.: Isolation of Chlorophyll *a*, Chlorophyll *b* and Pheophytin a on a Preparative Scale using High Speed Countercurrent Chromatography. (Poster). 41. Deutscher Lebensmittelchemikertag. Westfälische Wilhelms-Universität Münster, 10.-12.9. (2012). Abstract in Lebensmittelchemie 67(5), 114 (2013).

Castro-Benitez, M., Jerz, G., Winterhalter, P.: Isolation of cycloartane-type triterpenes from fruit peel of baby banana (*Musa acuminata*) by means of High-Speed countercurrent chromatography (Poster). 39. Deutscher Lebensmittelchemikertag. Stuttgart-Hohenheim, 20.-22.9. (2010). Abstract in Lebensmittelchemie 65(2), 31 (2011), erratum Lebensmittelchemie 65(4) 81 (2011).

Danksagungen

Die vorliegende Arbeit wurde im Rahmen des länderbezogenen Stipendienprogramms ALECOL durchgeführt und gründet sich auf die Kooperationsvereinbarung zwischen dem Deutschen Akademischen Austauschdienst (DAAD) und der Pontificia Universidad Javeriana Bogotá, Kolumbien (Stipendium-Kennziffer: A/06/32945).

Ich möchte auf Deutsch schreiben: **Dankeschön**; weil Deutschland **meine „Akademische Heimat“** ist. Ich lernte, als Doktorandin, im Institut für Lebensmittelchemie, TU-Braunschweig, was das Wort „Wissenschaft“ bedeutet. Ein großer Dank gilt allen, die mich während dieser Zeit unterstützt haben.

Lieber Herr Prof. Dr. Peter Winterhalter, meinen herzlichsten Dank, dass ich bei Ihnen meine Dissertation anfertigen durfte. Vielen Dank für das entgegengebrachte Vertrauen und die Unterstützung.

Le agradezco mucho Profesor Dr. P. Winterhalter por permitirme ser parte de su grupo de investigación y por darme la posibilidad de aprender. Usted es un gran ejemplo para mi de cómo debe ser un buen Profesor. Me llevo esta enseñanza en mi corazón y la voy a difundir en Colombia. Gracias por todo. Nunca olvidaré mis gratos momentos en el Instituto. Gracias a usted Alemania es maravillosa y siempre deberá recordar que para usted y mi afectuosa Evelyn, nuestro hogar en Colombia es vuestro hogar, por siempre.

Ein besonders großes Dankeschön an Frau Carola Balcke für ihre Hilfsbereitschaft, die vielen Korrekturen während der Jahre und die sorgfältige Durchsicht meiner schriftlichen Arbeit. Ich könnte nicht, ohne Ihre Unterstützung, hier etwas erreichen. Liebe Frau Balcke, ich danke auch für Ihre Freundschaft und Geduld.

Meinen Dank gilt ebenfalls Prof. Dr. Petra Mischnick und ihrer Arbeitsgruppe, inbesondere Frau Qimeng Zhang, Frau Julia Cuers, Herrn Marko Rother, Herrn Christian Bork, Frau Kristin Voiges und Frau Sheetal Gangula für die Unterstützung bei der Charakterisierung der Glycolipide und konstruktive Diskussionen.

Dem Arbeitskreis Winterhalter und dessen Ehemaligen gilt mein Dank für die nette Arbeitsatmosphäre. Vielen Dank Dr. Sebastian Tolle, Dr. Andreas Juadjur, Dr. Fabian Weber und Dr. Kathrin Ronneburg für Eure Geduld mit meinen Fragen!!

Ein besonderer Dank geht an Frau Stefanie Kuhnert, Frau Anne-Katrin Tschira, Herrn Ulf Stodt, Dr. Nils Kaiser und Frau Claudia Thräne für die vielseitige Unterstützung und tolle Zeit, insbesondere Dr. Tuba Esatbeyoglu, Dr. Stephanie Trebst, Dr. Yumen Hilal, Dr. Andrea Wilkens, Dr. Inga Unterieser, Dr. Christian Laue für die schönen Momente außerhalb der Uni. Frau Eva Schmalfuß, Frau Margret Brüggemann, Frau Rouba Horanni, Herrn Philipp Ewald, Herrn Recep Gök, Dr. Sebastian Macke und Frau Annika Burmeister danke ich für Eure Hilfe und vor allem Eure Begleitung.

Frau Tille-Lauckner, Frau Beate Maiwald, Frau Marita Baum, Frau Monika Messerer und Frau Silke Lehmann danke ich für die schnelle Lösung aller Probleme und auch für Eure besondere Freundschaft. Sie bleiben in meinem Herz.
Besonders hervorheben möchte ich:
- Dr. Peter Fleischmann danke ich für die konstruktiven Gespräche.
- NMR-Spektren: Dr. Kerstin Ibrom und Frau Petra Holba Schultz danke ich für die große Unterstützung.
- Herrn Oliver Willeke, Frau Amelie Wilde und Frau Mira Timpe danke ich für die praktische Unterstützung dieser Arbeit.
- Gäste: Un especial agradecimiento por el entusiasmo e invalubale apoyo que me brindaron durante vuestra estancia en el Instituto a Maria Muñoz (mi Maria), Aida Mezquida (mi Aida), Dr. Fernanda das Neves Costa (mi querida amiga y consejera), Dr. Monica Schwarz y Dr. Ana Maria Sanchez.
- Braunschweiger Wach- und Schließgesellschaft: Herr Thomas Kötz

Meiner lieber Familie: los adoro, y te agradezco **mi Umañosky** que me hayas apoyado en este camino, gracias a ti he llegado al final. Mi amor lindo, **Diego**, gracias por existir en nuestra vida. **Noche**, **Tobita y Mitsu**, nuestra amorosa y cálida compañía en Alemania. **Gracias.**

Zusammenfassung und Ausblick

Der Grad der Grünfärbung einer Banane wird durch Chlorophyll-Pigmente bestimmt und ist wichtig, um die Qualität im Zeitraum nach der Ernte festzustellen. Deshalb wurde in der vorliegenden Studie das Phänomen der Hyperpigmentierung, die an Schalen einiger Babybananen (*Musa acuminata AA Simmonds cv. Bocadillo*) aus Kolumbien beobachtet wurde, untersucht.

Wenn die Frucht das Stadium der grünen Reife erreicht, erscheinen schmale, grüne Streifen, die wieder verschwinden, sobald die Carotinoide zu den Hauptbestandteilen der Schale werden. Dieses Verschwinden kann mit einem Abbau des Chlorophylls in Zusammenhang gebracht werden, wie die Ergebnisse der vorliegenden phytochemischen Untersuchung zeigen.

Aus den Schalen von Babybananen wurden Chlorophyll *a* (Chl *a*), Chlorophyll *b* (Chl *b*) und Pheophytin *a* (Phy *a*) mittels Hochgeschwindigkeits-Gegenstromverteilungschromatographie (engl. High-speed countercurrent chromatography, HSCCC) und einem neuentwickelten Fließmittelsystem bestehend aus Hexan/EtOH/CH_2Cl_2/H_2O (6:2:4:2 *v/v/v/v*) isoliert. Dieses Fließmittelsystem ermöglicht die Ermittlung des Verhältnisses der Chlorophylle *a*/*b* sowie ihrer Derivate sowohl in Bananenschalen als auch in Gras und Spinat. Die Ergebnisse zeigten einen erheblichen Unterschied in der Pigmentzusammensetzung zwischen Babybananen mit Hyperpigmentierung und einer Babybananen-Kontrollgruppe.

Die Verhältnisse zwischen Chl *a*/*b* und Phy *a*/*b* in der Kontrollgruppe und in den hyperpigmentierten Bananen lassen darauf schließen, dass die Babybananen-Kontrollgruppe während des Abbauprozesses eine umgekehrte Chl-*b*-Biosynthese nutzt, um ausschließlich Chl-*a* zu produzieren, wohingegen Bananen mit Hyperpigmentierung kein Chl-*a* aufweisen und stattdessen Chl-*b* anreichern.

Laut aktuellen Veröffentlichungen finden Abbaumechanismen des Chlorophylls nicht nur in Chloroplasten/Gerontoplasten statt, sondern durch die Phäophorbid-*a*-Oxygenase (PaO) auch im Cytosol und in Vakuolen. Dieser

Vorgang führt zu einer Produktion von fluoreszierenden (Mc-FCC) und nicht-fluoreszierenden (NCCs) Chlorophyll-Kataboliten. Die Bevorzugung des Phäophorbids *a* gegenüber Phäophorbid *b* als Substrat von PaO liegt darin begründet, dass Phäophorbid *b* ein kompetitiver Inhibitor des PaO ist. Deshalb ist die Umsetzung des Chlorophylls *b* nötig, um Chlorophyll *a* zu erhalten.

Diese Ergebnisse könnten die Akkumulation von Chl-*b* in Babybananenschalen mit Hyperpigmentierung sowie das mit 0.86 geringere Verhältnis von Phy *a*/*b* im Vergleich zu 3.06 in der Kontrollgruppe erklären. Der Unterschied im Verhältnis von Phy *a*/*b* resultiert aus dem geringeren Anteil Phy *b* in der Babybananen-Kontrollgruppe verglichen mit dem hohen Gehalt von Phy *b* in den hyperpigmentierten Bananen.

Enzyme spielen während des Chlorophyllabbaus eine entscheidende Rolle, weshalb eine Methode zur Isolierung von Chlorophyllase-Enzym und- Proteinen in Babybananen angewandt wurde (siehe 4.3.6). Mittels SDS/PAGE wurden in den Extrakten aus Babybananenschalen ohne Hyperpigmentierung Proteinbanden in einem Bereich von 20 kD bis 37 kD gefunden. Aufgrund der Übereinstimmung sowohl mit der in der Literatur beschriebenen 25 kDa-Proteinbande als auch dem 35 kDa-Molekulargewicht des erhitzten Enzym-Proteins können diese der Chlorophyllase zugeordnet werden (Harpaz-Saad et al. 2007, Trebitsh et al. 1993). Weitere Studien sind nötig, um diese Ergebnisse mit dem Protein-Screening eines Extraktes aus hyperpigmentierten Babybananen zu vergleichen.

Mittels Spiral-Coil LSRCCC konnten 17 g eines Hexanextraktes aus hyperpigmentierten Babybananenschalen unter Verwendung des Fließmittelsystems Acetonitril/Hexan (1:1 *v*/*v*) fraktioniert werden. Chlorophyllderivate wurden im Elution-Extrusion-Modus eluiert (polar→unpolar). Diese Extraktionsmethode erhöht die Phäophytinisierung. Ferner zeigten Messungen mittels APCI-HPLC-MS, dass die Methode für derartige Inhaltsstoffe mit polaren und unpolaren Gruppen geeignet ist.

Weitere Untersuchungen via Spiral-Coil LSRCCC erscheinen sinnvoll, um bewerten zu können, wie sich das Verhältnis von Chlorophyll *a*/*b* unter

Anwendung der zweiten Extraktionsmethode verhält, die den vollständigen Chlorophyllabbau durch das neue Fließmittelsystem Hexan/EtOH/CH_2Cl_2/H_2O (6:2:4:2 *v/v/v/v*) verhindert.

Die Strukturaufklärung der in Fraktion 14 der Spiral-Coil LSRCCC-Trennung von hyperpigmentierten Babybananenschalen enthaltenen Tocotrienole durch 1D- und 2D-NMR ist wichtig, da diese Substanzen in der Kontrollgruppe nicht vorkommen.

Die vorläufigen Vermutungen wurden bekräftigt durch die Detektion der Hauptderivate des Chlorophylls in hyperpigmentierten Babybananenschalen während der Untersuchungen mittels Spiral-Coil LSRCCC. Hierbei handelte es sich um Pyrophäophorbide, welche mit Sterinen/Sterolen verestert waren (siehe 2.3.3). Während des Chlorophyll-Abbaus findet eine Abspaltung von Phytol statt, welches angereichert wird und gemäß den Veröffentlichungen von Collakova und DellaPenna (2003) sowie DellaPenna und Pogson (2006) zu Tocopherolen und Tocotrienolen umgewandelt werden kann. Eine Synthese von Tocopherolen findet ausschließlich in Organismen statt, die Photosynthese betreiben.

Die Anwesenheit von Triterpenalkohol-ferulaten in Reiskleieöl wurde nach einer Fraktionierung durch HSCCC bereits in der Literatur beschrieben (Angelis et al. 2011; Liu et al. 2013). In der Spiral-Coil LSRCCC Fraktion 14 konnten mit Hilfe von APCI-HPLC-MS sowohl 25-Hydroxy-24-methylcycloartenylferulat sowie mittels 1D- und 2D-NMR-Experimenten Cycloartenyl-*trans*-ferulat identifiziert werden (siehe 2.3.4.1, 2.3.4.2). Die oben genannten Quellen berichten weiterhin, dass unter dem Namen γ-Oryzanol ein funktionelles Speiseöl vertrieben wird, welches als Nebenprodukt der Reiskleie hohe Gehalte an Sterinen/Sterolen, Triterpenalkohol-ferulaten und Vitamin E (Tocopherole und Tocotrienole) aufweist. Demzufolge stellen Babybananenschalen mit Hyperpigmentierung ein wertvolles Ausgangsmaterial für Produkte mit antioxidativen und hypocholesterinämischen Eigenschaften dar (Scavariello und Arellano 1998; Islam et al. 2008).

Bei der phytochemischen Analyse von Babybananenschalen wurde das Glycolipid O-α-D-Gal*p*(1''→6')-O-β-D-Glu*p*(1'→3)-2,1-diacyl-L-glycerol entdeckt, welches damit zum ersten Mal in einer höheren Pflanzenart nachgewiesen wurde (siehe 2.1.2). Des Weiteren wurden die Strukturen von Phosphatidylcholin (Lecithin), Phosphatidylethanolamin, Sulphoquinovosyldiacylglycerol sowie molekulare Spezies des Glucocerebrosids mit Hilfe von 1D-, und 2-D-NMR-Spektroskopie aufgeklärt. Diese Verbindungen wurden im Rahmen dieser Arbeit erstmalig in Bananen nachgewiesen.

Es ist wichtig zu beachten, dass Carotinoide keine bedeutende Rolle in Bezug auf das Phänomen der Hyperpigmentierung spielen, da sich ihre Gehalte in beiden Bananenarten ähneln. Allerdings ermöglicht das zweite neue Fließmittelsystem Hexan/EtOH/$CHCl_3$/H_2O (6:2:4:2 *v*/*v*/*v*/*v*) die Isolierung von Xanthophyllen aus Früchten und Pflanzen, wovon weitere Forschungsarbeiten profitieren könnten.

Forschungsansätze für die nahe Zukunft bestehen in der gründlichen Analyse weiterer Bestandteile der HSCCC-Fraktionen, welche aus methanolischen Extrakten der hyperpigmentierten Babybananenschalen und der Kontrollgruppe gewonnen wurden. Hierdurch soll das Vorkommen polarer Derivate des Chlorophylls, wie z. B. ein roter Chlorophyllkatabolit (engl. red chlorophyll catabolite, RCC), neue fluoreszierende Chlorophyllkatabolite (engl. fluorescent chlorophyll catabolites, FCCs) und nicht-fluoreszierende Chlorophyllkatabolite (engl. nonfluorescent chlorophyll catabolites, NCCs), erklärt werden. Anschließend sollte der Fokus auf die Erforschung des Hyperpigmentierungsphänomens an frischen kolumbianischen Babybananen mittels HSCCC und Spiral-Coil LSRCCC und unter Anwendung der im Rahmen dieser Arbeit entwickelten Methoden gelegt werden.

“May all being find peace, joy, and liberation”

H.H. Gyalwa Karmapa Orgyen Trinley Dorje

To Prof. Emeritus Eliezer E. Goldschmidt,
Camilo and Diego

TABLE OF CONTENTS

	Introduction	1
1	**GENERAL CONCEPTS**	3
1.1	**Baby Banana (*Musa acuminata* AA Simmonds cv. Bocadillo)**	4
1.1.1	Taxonomic Classification of Bananas (*Musa acuminata*)	4
1.1.2	Plant morphology	5
1.1.3	Pre-harvest	8
1.1.4	Post-harvest	10
1.1.4.1	*Hyperpigmentation phenomenon*	*12*
1.2	**Chlorophyll degradation**	14
1.3	**High-Speed Countercurrent Chromatography**	24
1.4	**Spiral-Coil Low-Speed Rotary Countercurrent Chromatography (Spiral-Coil LSRCCC)**	27
2	**RESULTS AND DISCUSSION**	29
2.1	**Phytochemical profile of Baby Banana control peels**	30
2.1.1	Phosphatidylcholine (Lecithin)	31
2.1.2	Glycosyldiacylglycerolipids	38
2.1.2.1	*O-α-D-Galp (1''→ 6')- O-β-D-Glup (1'→ 3)- 2, 1-diacyl-L-glycerol (GGDG)*	*39*
2.1.2.2	*O-β-D-Galp(1'''-3)-2, 1 diacyl-L-glycerol (MGDG)*	*55*
2.1.2.3	*Compositional analysis of the glycolipid GGDG and MGDG*	*70*
2.1.2.4	*Summary*	*75*
2.1.3	Molecular species of glucocerebroside	79
2.1.4	Sulphoquinovosyl-diacylglycerol (SQDG)	88

2.1.5 Phosphatidylethanolamine (PE) 90
2.1.6 Ceramide aminoethylphosphonate (CAEP) 92
2.1.6.1 Summary *93*
2.1.7 Linoleic acid 94
2.1.7.1 Summary *103*
2.1.8 Lutein 104
2.1.9 Violaxanthin-di-laurate and β-Carotene isomers 110
2.1.9.1 Summary *123*
2.1.10 4-Epi-cycloeucalenone and 4-Epi-cyclomusalenone 127
2.1.11 ß-Sitosterol 134
2.1.11.1 Summary *138*
2.1.12 Pheophytin-a 141
2.1.13 Summary 152

2.2 Optimization of the solvent system for the separation of chlorophylls and derivatives by means of High-Speed Countercurrent Chromatography in Baby Banana peels, spinach and grass 154
2.2.1 Experimental Design 154
2.2.2 Isolation of chlorophylls and derivatives from spinach by HSCCC 167
2.2.3 Role of dichloromethane and chloroform as stationary phase in the solvent system for the isolating of chlorophylls and xanthophylls from plant extracts by HSCCC 178
2.2.4 Chlorophylls *a*/*b* ratio and derivatives in Baby Banana peels and other plants by HSCCC 184

2.3 Preparative Spiral-Coil Low Speed Rotary Countercurrent chromatography of Baby Banana peels (*Musa acuminata*) with hyperpigmentation. 190
2.3.1 APCI-HPLC-MS-MS analysis of Spiral-Coil-LSRCCC fractions from Baby Banana peels with hyperpigmentation 194
2.3.2 Identification of polar compounds in Spiral-Coil-LSRCCC 204

2.3.3 Identification of chlorophyll derivatives esterified with sterols in Spiral-Coil-LSRCCC 207
2.3.4 Spiral-Coil-LSRCCC of Baby Banana peels with hyperpigmentation: comparison with HSCCC of Baby Banana control 210
2.3.4.1 Elucidation of tocopherols and tocotrienols in Fraction 14 of Spiral-Coil-LSRCCC separation from Baby Banana peels with hyperpigmentation extract 217
2.3.4.2 Elucidation of Triterpene Alcohol Ferulates in Fraction 14 of Spiral-Coil-LSRCCC separation from Baby Banana peels with hyperpigmentation extract 229
2.3.5 Summary 233

3 SUMMARY AND OUTLOOK 235

4 MATERIAL AND METHODS 239
4.1 Plant Material and Chemicals 240
4.1.1 Plant Material 240
4.1.2 Chemicals and Solvents 240

4.2 Equipments and Parameter 242
4.2.1 High-Performance Liquid Chromatography (HPLC) 242
4.2.1.1 Jasco-System (HPLC-DAD) 242
4.2.1.2 Knauer-System (preparative) – Equipment I 242
4.2.1.3 Knauer-System (preparative) – Equipment II 242
4.2.1.4 Analytical Columns 243
4.2.1.5 Preparative Columns 243
4.2.1.6 Solvent System and Gradients of HPLC – DAD 243
4.2.1.7 Solvent System and Gradients of Preparative HPLC 244
4.2.2 Mass spectrometry 245
4.2.2.1 APCI-HPLC-MS-MS 245
4.2.2.2 Column APCI-HPLC-MS-MS 245

4.2.2.3 Parameter Mode APCI-HPLC-MS-MS *245*

4.2.2.4 Solvent system and gradient of APCI-HPLC-MS *245*

4.2.3 High-Speed Countercurrent Chromatography (HSCCC) 246

4.2.3.1 Solvent System of High-Speed Countercurrent Chromatography (HSCCC) *246*

4.2.4 Gas Chromatography 247

4.2.4.1 GC-MS I *247*

4.2.4.2 GC-MS II *247*

4.2.4.3 GC-MS III *247*

4.2.5 Spiral-Coil Low-Speed Rotary Countercurrent Chromatography (Spiral-Coil LSRCCC) 248

4.2.5.1 Solvent system for Spiral-Coil LSRCCC *248*

4.2.6 Nuclear Magnetic Resonance Spectroscopy 248

4.3 Methods 249

4.3.1 Extraction Methods 249

4.3.1.1 First Extraction Method *249*

4.3.1.2 Second Extraction Method *249*

4.3.2 Thin Layer Chromatography (TLC) 250

4.3.2.1 System 1 *250*

4.3.2.2 System 2 *250*

4.3.3 Compositional analysis of glycolipids 250

4.3.3.1 Analysis of fatty acid components by Gas chromatography–mass spectrometry (GC-MS) *250*

4.3.3.2 Sugar composition of glycolipids (SCG) *251*

4.3.4 Isolation of pheophytin from methanol phase of Baby Banana peels by means of Normal Phase Chromatography 252

4.3.5 Isolation of carotenoids from acetone extract of Baby Banana peels with hyperpigmentation by means of Normal Phase Chromatography 252

4.3.6 Partial isolation of chlorophyllase and proteins from flavedo of Baby Banana peels 253

4.3.6.1 SDS/PAGE condition *254*

5 BIBLIOGRAPHY 255

List of Figures

Figure 1-1. Baby Banana cultivation in Cundinamarca, a central region of Colombia (South America). 7

Figure 1-2. Baby Bananas (*Musa acuminata AA Simmonds cv*." Bocadillo") from Colombia at different stages of ripening after being harvested. 7

Figure 1-3. Commercial Baby Banana growing areas in Colombia, in western Antioquia Department, in central territory, and in the eastern Santander Department (Belalcázar, 1991). 9

Figure 1-4. Exportations from Colombia ranking in US $ (millions) for 2013 (left) and receiving countries in Europe (right). 9

Figure 1-5. Post-harvest of Baby Bananas in green stage before being exported (left). Control color chart of Bananas used during the post-harvest marketing. 10

Figure 1-6. Baby Banana with hyperpigmentation (HP) (left), and without hyperpigmentation (Control), (right). 12

Figure 1-7. Baby Banana with hyperpigmentation at different stages of ripening during 10 days after being harvested. 13

Figure 1-8. Structural formulas and nomenclature of chlorophylls and their derivatives (Huang et al. 2008). 15

Figure 1-9. Nomenclature of the porphyrins related to Chl a and the isomer Chl a' (Aronoff 1966). 16

Figure 1-10. Chlorophyll breakdown pathway in higher plants (first stage) (Hörtensteiner 2006). 17

Figure 1-11. Product of the pheophorbide a reaction to red chlorophyll catabolite (RCC). (Kräutler et al. 1991, 1992, 2012). 18

Figure 1-12. Reduction of red chlorophyll catabolite (RCC) to produce the "primary" fluorescent chlorophyll catabolite (*p*FCC or its C1 epimer, *epi*-*p*FCC) in senescent leaves and ripening fruit (Kräutler and Hörtensteiner 2006). 20

Figure 1-13. Fluorescent catabolites (*Mc*-FCCs) in extract of the peels of freshly ripe bananas (Thomas et al. 1989; Moser et al. 2012). 21

Figure 1-14. Nonfluorescent catabolites (*Mc*-NCCs) identified in an extract of the peels of ripe banana (Moser et al. 2012; Mühlecker and Kräutler 1996; Mühlecker et al. 1997). 23

Figure 1-15. Preparative triple-coil planetary motion of separation column in High-Speed Countercurrent Chromatography (HSCCC). 24

Figure 1-16. Schematic drawing of motion and distribution of two phases in the spiral column undergoing type J- planetary motion in High-Speed Counter Current Chromatography (Ito and Conway 1996). 25

Figure 1-17. Schematic drawing of a High-Speed Countercurrent Chromatography (Sutherland, 1987) 26

Figure 1-18. Assembly of Spiral-Coil Low Speed Rotary Countercurrent chromatography (Spiral-Coil LSRCCC). 27

Figure 2-1. HSCCC chromatogram of 405.5 mg of an extract from Baby Banana peels monitored at 440 nm using elution and extrusion mode. 30

Figure 2-2. Fraction 7. Left: RP-18 TLC and Silica gel screening of target fraction 7 from HSCCC elution phase containing 62.25 mg of lipids. (a) Silica gel TLC. (b) RP-18 TLC 363 nm. (c) RP-18 TLC developed plate with p-anisaldehyde stain. Right: Separation of fraction 7 by HPLC-reversed phase system. 31

Figure 2-3. Chemical structure of phosphatidylcholine. Chemical shift of HSQC correlation shows numbered carbons and protons that confirm the elucidated data. 32

Figure 2-4. 600 MHz ^{13}C-NMR spectrum of phosphatidylcholine in CD_3OD. 33

Figure 2-5. ^{1}H-NMR and ^{13}C-NMR HSQC spectra of phosphatidylcholine (hydrophilic region). The spectral region of hydrophilic portion between 50-75 ppm resonances of ^{13}C and the ^{1}H signals represents the phosphate group esterified with the OH-group of choline. 35

Figure 2-6. One dimensional ^{31}PNMR spectra of phosphatidylcholine (PTC). 36

Figure 2-7. ^{13}C and DEPT NMR spectra of methyl belongs to hydrophilic section of the PTC corresponding to $(CH_3)_3N$. 37

Figure 2-8. Positive-ion APCI mass spectra of 1-2-dilinoleyl glyceryl-phosphorylcholine. Intensity [mAU] depicts the percentage relative abundance plotted against *m/z* values between 150 and 1500. The peak *m/z* 780.4 was identified as the molecular ion peak and three daughter ions at *m/z* 663, *m/z* 618.4 and *m/z* 391.0 result from the loss of choline and Phosphorous moieties and the fragmentations of the linolenic acid. 38

Figure 2-9. Structure relevant long-range HC-correlation in the HMBC of *O*-α-D-Gal*p* (1''→ 6')- *O*-β-D-Glu*p* (1'→ 3)- 2, 1-diacyl-L-glycerol. (A) Glucose HMBC; (B) Galactose HMBC. 40

Figure 2-10. Structure relevant correlation in the COSY of *O*-α-D-Gal*p* (1''→ 6')- *O*-β-D-Glu*p* (1'→ 3)- 2, 1-diacyl-L-glycerol in CD_3OD. (A) Glucose COSY; (B) Galactose COSY. 42

Figure 2-11. The 600 MHz COSY spectrum of *O*-α-D-Gal*p* (1''→ 6')- *O*-β-D-Glu*p* (1'→ 3)- 2, 1-diacyl-L-glycerol in CD_3OD. 43

Figure 2-12. The 600 MHz 2D NOESY spectrum of O-α-D-Gal*p* (1''→ 6')- O-β-D-Glu*p* (1'→ 3)- 2, 1-diacyl-L-glycerol in CD_3OD with relevant enhancements used to define the stereochemistry of the molecule. 44

Figure 2-13. Relevant NOEs enhancements used to define the stereochemistry of *O*-α-D-Gal*p* (1''→ 6')- *O*-β-D-Glu*p* (1'→ 3)- 2, 1-diacyl-L-glycerol in CD_3OD (A) Glucose NOESY (B) Galactose NOESY. 46

Figure 2-14. GC-MS chromatogram and mass spectrum from the acyl moiety from *O*-α-D-Gal*p* (1''→ 6')- *O*-β-D-Glu*p* (1'→ 3)-2, 1-diacyl-L-glycerol after the derivatization. The resulting methyl ester derivatives corresponded to a linolenic acid (*m/z* 292) and to a palmitic acid (*m/z* 270), and

retention times of 45.32 and 36.07 min, respectively. The chromatogram of the methyl ester derivatives depicted the occurrence of few other peaks possibly corresponding to oleic and linoleic acids in low proportion. 48

Figure 2-15 b. The mass spectra for O-α-D-Gal*p* (1''→ 6')- O-β-D-Glu*p* (1'→ 3)-2, 1 -L-diacyl- glycerol (GGDG) by HPLC-APCI-MS and the proposed fragmentation schema with 18:3/18:3 linolenic acid as acyl moieties (Yamauchi et al. 2001; Yamauchi 2005; Benning et al. 1995) (Figure 2-15a). 51

Figure 2-16. The identification of resonances corresponding to methyl signals at δ 14.44/0.80 and δ 14.71/0.87 ppm from palmitic and linolenic acid, respectively, in the ^{1}H spectrum of O-α-D-Gal*p* (1''→ 6')- O-β-D-Glu*p* (1'→ 3)-2, 1 -L-diacyl-glycerol (GGDG) in fraction 4. 52

Figure 2-17. Relevant NOEs enhancements used to define the stereochemistry of ω-3 linolenic acid and palmitic acid in the GGDG structure.(Above) Linolenic acid-C-2 Glycerol and palmitic acid-C-1-Glycerol NOEs enhancements. (Below) Relevant NOEs enhancements of H-11 from linolenic acid-C-2-Glycerol. 53

Figure 2-18. Possible arrangement of the substituents in *O*-α-D-Gal*p* (1''→ 6')- *O*-β-D-Glu*p* (1'→3)-2-linoleyl, 1-palmitoyl-L-glycerol according to 2D NOESY and COSY spectra. 54

Figure 2-19. Structure relevant long-range HC-correlation in the HMBC of *O*-β-D-Gal*p* (1'''-3)-2, 1 diacyl-L-glycerol (MGDG). 56

Figure 2-20. The HSQC long-range correlation spectrum shows the relevant resonances of the structure (1) *O*-β-D-Gal*p*(1'''-3)-2, 1 diacyl-L-glycerol (MGDG) such as the signals of C-2'-2''' Gly 71.79 and 71.82, respectively (upper left); C-1'-1''' Gly 63.97 overlapped peak (upper right) and C-3'''gly into the spectrum (The assignments from C-1''' to C-6''' are pointed with red circles). 58

Figure 2-21. Relevant NOEs enhancements used to define the stereochemistry of the β-D-Gal*p* (1'''→ 3)-2, 1-diacyl-L-glycerol in fraction 6 of the preparative RP-18 –HPLC separation from fraction 7 of HSCCC in Baby Banana peels. 61

Figure 2-22. ^{13}C chemical shift resonances corresponding to C-1 (A) and C-2 (B) of the linolenic acid (Ln), linoleic acid (L) and palmitic acid (P) to illustrate as the sequence of the distance was constant during the 1D/2D NMR experiments. 64

Figure 2-23. GC-MS chromatogram and mass spectrum from the acyl moiety from O-α-D-Gal*p* (1''→ 6')-O-β-D-Glu*p* (1'→ 3)- 2, 1-diacyl-L-glycerol (GGDG) and O-β-D-Gal*p*(1'''-3)-2, 1 diacyl-L-glycerol (MGDG) after the derivatization in fraction 6. The resulting methyl ester derivatives corresponded to methyl linolenoate, methyl linoleate and methyl palmitate. The occurring of the small peak could be linked to the glycerol moiety. 66

Figure 2-24. APCI-MS spectra for O-α-D-Gal*p* (1''→ 6')- O-β-D-Glu*p* (1'→ 3)- 2, 1-diacyl-L-glycerol (GGDG) (above) and *O*-β-D-Gal*p*(1'''-3)-2, 1 diacyl-L-glycerol (MGDG) in fraction 6 (below). 69

Figure 2-25. Summary of the fragment ions observed for *O*-α-D-Gal*p* (1''→ 6')- *O*-β-D-Glu*p* (1'→ 3)- 2, 1-diacyl-L-glycerol (GGDG) by means ESI-MS and a proposed fragmentation. 71

Figure 2-26. Gas chromatogram of alditol acetates of glucose standard from methyl cellulose, GGDG and their co-injection. Comparison in separated chromatograms (above) and comparison between the retention times where the chromatograms are overlapped (below). 73

Figure 2-27. Gas chromatogram of alditol acetates of galactose standard, GGDG and their co-injection. Comparison in separated chromatograms (above) and comparison between retention times where the chromatograms are overlapped (below). 74

Figure 2-28. Total ion chromatogram from *O*-α-D-Gal*p* (1''→ 6')- *O*-β-D-Glu*p* (1'→ 3)- 2, 1-diacyl-L-glycerol (GGDG) by GCL-MS from alditol acetate GGDG. 75

Figure 2-29. Chemical structure of glucocerebroside is characterized as (4*E*, 8*E*) –N-2'–hydroxylinolenoyl-1-O-β–D-glucopyranosyl-4, 8-sphingadienine by 1D/2D-NMR spectroscopy (^{1}H, ^{13}C, ^{1}H/^{1}H-COSY, HSQC, HMBC, NOESY) in fraction 8. 79

Figure 2-30. Partial ^{1}H NMR spectra (A) Amide characteristic ^{1}H proton signal of the ceramide, which resonances are in the region between at δ 7.52 and δ 7.62 (B) Identification of methyl signals at δ 0.93 and 0.85 (iso-propyl terminus) belonging to ceramides in fraction 8. These relevant enhancements support the presence not only of the glucocerebroside (1) elucidated as (4*E*, 8*E*) –N-2' –hydroxylinolenoyl-1-O-β–D-glucopyranosyl-4, 8-sphingadienine but also a homologous or related compound. 82

Figure 2-31. APCI-MS mass fragmentation pattern of (4*E*, 8*E*)–N-2' –hydroxylinolenoyl-1-O-β–D-glucopyranosyl-4, 8-sphingadienine, glucocerebroside (1). 83

Figure 2-32. Positive-ion APCI mass spectra of (4*E*, 8*E*)–N-2'–hydroxylinolenoyl-1-O-β–D-glucopyranosyl-4, 8-sphingadienine, glucocerebroside (1). Intensity [mAU] depicts the relative percentage abundance plotted against *m/z* values between 150 and 1500. The peak $[M+H]^{+}$ 752.4 *m/z* was identified as a molecular ion peak; the fragmentation pattern showed the ceramide moiety at *m/z* 572.3 and the sphingoid-(H_2O) moiety at *m/z* 262 from glucocerebroside (Riaz et al. 2013; Yamauchi 2005; Kasumov et al. 2010). 83

Figure 2-33. GC-MS chromatogram from the acyl moiety in fraction 8 after the derivatization. The resulting methyl ester derivatives corresponding to methyl linolenoate at *m/z* 292 in 45.32 min, methyl linoleate at *m/z* 294 in 43.88 min and methyl palmitate at *m/z* 270 in 36.7 min and the presence of a new peak that represents the sphingoid moiety at *m/z* 298 in 42 min. 84

Figure 2-34. Mass spectrum corresponding to the sphingoid moiety [$R^{1}CH(OH)CH(NH_2)CH_2$] belonging to glucocerebroside (1) (Yamauchi et al. 2001; Riaz et al. 2013). 85

Figure 2-35. (Above) APCI-MS fragmentation pattern of glucocerebroside (2) identified as (8*E*)–N-2'hydroxydocosanoyl-1-O-β–D-glucopyranosyl-4-hydroxy-8-sphingaenine; (below) APCI-MS data of glucocerebroside (2). 86

Figure 2-36. Positive-ion APCI mass spectra of (8*E*)–N-2' –hydroxydocosanoyl-1-O-β–D-glucopyranosyl-4-hydroxy-8-sphingaenine, glucocerebroside (2). Intensity [mAU] depicts the percentage relative abundance plotted against *m/z* values between 150 and 1500. The peak $[M+H]^{+}$ 816.4 *m/z* was identified as the molecular ion peak and the fragmentation pattern showed the ceramide moiety at *m/z* 654 and the sphingoid-(H_2O) moiety at *m/z* 262 from the sphingoid. Two types of

fragmentation have been observed and they are indicated in the mass spectra with a circle and a rectangle to differentiate each other (Riaz et al. 2013; Yamauchi 2005; Kasumov et al. 2010). 87

Figure 2-37. Chemical structure of O-β-D-Qui*p*-6-sulphono (1' ↔ 3)-2, 1—diacyl-L-glycerol, sulphoquinovosyl-diacylglycerol (SQDG) elucidated in fraction 8. 88

Figure 2-38. ^{31}P spectrum from fraction 9 indicated the occurrence of Phosphorous element at δ 0.73 which corresponds to phophatidylethanolamine (PE) and phosphathidylcholine (PC) in lower proportion, and also at δ 1.49 to the ceramide-aminoethylphosphonate (CAEP). 90

Figure 2-39. Chemical structure of phosphatidylethanolamine (1, 2- dilinoleoylphosphatidyl-ethanolamine) and chemical shift of HSQC correlation with numbering of carbons and protons according to literature data (Sobolev et al. 2005). 91

Figure 2-40. ^{13}C spectrum of fraction 9 which showed two resonances at δ 41.759 and 41.712 suggesting the occurrence of two Phosphorous moieties in the fraction belonging to phosphatidylethanolamine (PE). 92

Figure 2-41. Tentative structure of ceramide aminoethylphosphonate (CAEP) elucidated in fraction 9 by HMBC, COSY and NOESY experiments, in concordance with literature data (de Souza et al. 2007). 93

Figure 2-42. (Above) RP-18 TLC (Thin Layer Chromatography) in MeOH (100%) of linoleic acid in fraction 6 that corresponds to the tubes [82-89] in elution mode. (Below) Spiral coil LSRCCC chromatogram of Baby Banana peels with hyperpigmentation (HP). Fraction 6 in elution mode contains linoleic acid which was isolated and identified by 1/D and 2/D NMR experiments. 96

Figure 2-43. 600 MHz ^{1}H-NMR spectrum of linoleic acid in CD_2Cl_2 (Left); 150 Hz DEPT spectrum of linoleic acid in CD_2Cl_2 (Right). 97

Figure 2-44. 600 MHz ^{13}C-NMR spectrum of linoleic acid in CD_2Cl_2. The olefinic, allylic and carbonylic regions are precisely identified in the spectrum such as the 18 carbons which conform the chemical structure of the linoleic acid (Hatzakis et al. 2011; Zamora et al. 2002). 97

Figure 2-45. Structure relevant HC-correlation in the HSQC (Heteronuclear single-quantum correlation) and the HMBC (Heteronuclear multiple bond correlation) from linoleic acid 18:2 (Δ9Z, 12 Z) in fraction 6. HSQC and HMBC analysis were in agreement with literature data (Vlahov 2009; Hatzakis et al. 2011; Zamora et al. 2002; Gunstone 1990; Gunstone 1993). 99

Figure 2-46. The 600 MHz 2D HMBC spectrum of linoleic acid 18:2 (Δ9Z, 12Z) shows the enhancements between olefinic and allylic regions which support the chemical structure of an unsaturated fatty acid in fraction 6. 99

Figure 2-47. The 600 MHz COSY spectrum of ω-6 linoleic acid in fraction 6 from spiral coil–LSRCCC separation of Baby Banana peels with hyperpigmentation (CD_2Cl_2). 100

Figure 2-48. Relevant NOE enhancements used to define the stereochemistry of ω-6 linoleic acid in fraction 6 from spiral coil–LSRCCC separation of Baby Banana peels with hyperpigmentation. The red circles indicate the correlation between three relevant resonances between H-18 at δ 0.9 with H-3 at δ 1.65, between H-2 at δ 2.33 with H-14 at δ 2.06 and between H-11 at δ 2.81 with H-4,7 at δ 1.34 which illustrate that the molecule could be twisted (600 MHz, CD_2Cl_2). 101

Figure 2-49. Final stereochemistry proposal of the ω-6 linoleic acid (18:2, Δ9*Z*, 12Z) according to NOESY and COSY experiments in fraction 6 from spiral coil–LSRCCC separation of Baby Banana peels with hyperpigmentation (CD_2Cl_2). 101

Figure 2-50. HPLC-APCI-MS-MS analysis (positive ion mode) of fraction 6 from spiral coil-LSRCCC of Baby Banana peels. (Above) Linoleic acid is the major fatty acid with *m/z* 278 and traces of arachidic acid (20:0) with *m/z* 295, in 3.0 min (Below). Traces of pheophytin *b* and hydroxypheophytin *a* with *m/z* 885 and 887, respectively at 22.4 min (displays fluorescence at UV 423 and 677 nm) in DAD-contour-plot (Jakab et al. 2002; Holčapek et al. 2003). 102

Figure 2-51. HSCCC chromatogram of Baby Banana peels with hyperpigmentation (HP) from the methanol extract. Fraction 3 in elution mode contained 12.4 mg of lutein which was identified by 1/D and 2/D NMR experiments in CD_2Cl_2. 105

Figure 2-52. RP-18 TLC screening, under white light, of tubes corresponding to fraction 3 from HSCCC elution. 105

Figure 2-53. Structure of (all-E)-lutein (3R, 3′R, 6′R)-*β*, *ε*-carotene-3, 3′-diol isolated from Baby Banana peels with hyperpigmentation by means of High Speed Countercurrent Chromatography (HSCCC). 106

Figure 2-54. The 600 Hz COSY spectrum (left) and ^{13}C spectrum (right) of lutein isolated from Baby Banana with hyperpigmentation by HSCCC in CD_2Cl_2. 106

Figure 2-55. Structure relevant long-range HC-correlation in the HMBC and HSQC of lutein (3R, 3′R, 6′R)-β, ε-carotene-3, 3′-diol from Baby Banana peels in CD_2Cl_2 108

Figure 2-56. HPLC-APCI-MS-MS spectra (positive ion mode) of a quasimolar ion at *m/z* 551 [M+H-H_2O] corresponding to lutein isolated in fraction 3 from Baby Banana peels with hyperpigmentation (below), at 16.2 min according to the chromatogram (middle), at 420, 444 and 472 nm as the UV absorption maxima (above), in concordance with literature data (de Rosso and Mercadante 2007; Mercadante et al. 1997; Britton et al. 1995; Gross et al. 1973a; Subagio et al. 1996). 109

Figure 2-57. HSCCC separation of the "acetone extract", solvent system: hexane/EtOH/Water/ (6/5/2), flow rate 3.5 mL/min in elution and 6.0 mL/min in extrusion mode, elution mode ” head to tail”, detection at λ 220 nm. 111

Figure 2-58. (A) Normal phase chromatography of 100 mg of HSCCC fraction 12; (B) TLC plate of silica gel of fraction 1 corresponding to tubes [9-12] in the normal phase separation; (C) TLC plate of silica gel of fraction 1 corresponding to tubes [9-12] in the normal phase separation, after been developed with anisaldehyde as chromogenic agent. 112

Figure 2-59. ^{13}C NMR spectrum of fraction 1 obtained by means of normal phase chromatography from the "acetone extract" of Baby Banana peels with hyperpigmentation. The ^{13}C chemical shifts in the spectrum represent the resonances of carotenoids, carotenoid ester, fatty acid and triterpenoids which were gathered according to ^{1}H, HSQC, HMBC, COSY and NOESY experiments. 113

Figure 2-60. HMBC spectrum at 600 MHz confirms the multiple-bond correlation between C-1 from fatty acid at (δ 173.61-173.69) with H-3 (δ 4.45-4.39) of ß-violaxanthin identified by means of 1/D, 2/D NMR experiments and HPLC-APCI-MS-MS mass spectrometry, in fraction 1 from an acetone extract of Baby Banana peels with hyperpigmentation (HP). 114

Figure 2-61. HSQC spectrum at 600 MHz confirms the single quantum correlation of two ester bonds at δ 78.42-80.40 with protons at δ 4.39-4.45, whose resonances could correspond to ester bonds between C-3 of ß-violaxanthin and C-1 of fatty acids. 115

Figure 2-62. HPLC–APCI–MS-MS chromatogram (below) and contour-plot of fraction 1 obtained in a normal phase chromatography separation from the "acetone extract" of Baby Banana peels. Two peaks at 25.4 and 25.5 min in the chromatogram represent two carotenoids in fraction 1 with absorptions between λ 400- 500 nm. 115

Figure 2-63. UV-spectrum of a violaxanthin-di-laurate recorded on line during the HPLC-APCI analysis by using a photodiode-array detector with three absorption maxima at 422, 446, 472 nm (above) and the mass spectrum with a quasimolecular ion at *m/z* 964 $[M+H]^+$ (below), in fraction 1, from acetone extract of Baby Banana peels with hyperpigmentation (van Breemen et al. 2012; Kohler 1995). 117

Figure 2-64. Positive ion APCI mass spectra of violaxanthin-di-laurate (C 12:0, C 12:0) and the pattern of fragmentation. The data was in concordance with the literature (van Breemen et al. 2012; Breithaupt 2004; Schweiggert et al. 2005). 118

Figure 2-65. Relevant long-range HC-correlation in the HMBC, HSQC and COSY of (3*S*, 3 *S')*-violaxanthin-di-laurate (C 12:0;C 12:0) elucidated in fraction 1 and obtained by means of a normal phase chromatography from acetone extract of Baby Banana peels with hyperpigmentation. The data was in agreement with the literature (Englert et al. 1977). 118

Figure 2-66. ^{1}H spectra at 600 MHz of the olefinic region of the carotenoids in fraction 1. The brakets gather the ^{1}H resonances of each group of protons in the carotenoids according to the position in the isoprenoid chain between H-8 and 8'. The data was in agreement with literature (Molnár et al. 1997; Maoka and Akimoto 2011; Putzbach et al. 2005a; Putzbach et al. 2005b; Strohschein et al. 1997). 119

Figure 2-67. UV-spectra of cis-neo-β-carotene recorded on line during the HPLC-APCI analysis by using a photodiode-array detector at 25.3 min with four absorption maxima at 335, 420, 443, 473 nm (above) and mass spectrum with a base peak of *m/z* 537 $[M+H]^+$ (below) in fraction 1 from the acetone extract of Baby Banana peels with hyperpigmentation (Gross et al. 1973a; Lacker et al. 1999; Maoka et al. 2002; de Rosso and Mercadante 2007). 120

Figure 2-68. Schema of positive ion APCI mass spectral fragmentation of cis-neo–ß-carotene (15-cis) and the pattern of fragments according to literature data (van Breemen et al. 2012; Weller and Breithaupt. 2003; Breithaupt and Schwack 2000; Subagio et al. 1996; Mercadante et al. 1997; Hu et al. 1997; Lacker et al. 1999; Tsukida and Saiki 1982). 121

Figure 2-69. UV spectrum of 15-cis ß-carotene recorded on-line during the HPLC-APCI –MS analysis at 25.5 min by using a photodiode-array detector with three maxima at 335, 448, 475 nm (above) and mass spectrum with a base peak of *m/z* 537 [M+H]+ (below) in fraction 1 from the acetone extract of Baby Banana peels with hyperpigmentation (Hu et al. 1997; Lacker et al. 1999). 122

Figure 2-70. Schema of positive ion APCI mass spectral fragmentation of 15-cis ß-carotene and the pattern of fragments according to literature data (van Breemen et al. 2012; Weller and Breithaupt

2003; Breithaupt and Schwack 2000; Subagio et al. 1996; Mercadante et al. 1997; Hu et al. 1997; Lacker et al. 1999; Kohler 1995). 122

Figure 2-71. HSCCC chromatogram of Baby Banana n-hexane phase extract (1.0 g) in elution mode with a solvent system (n-hexane/MeOH), (2:1). Two positional isomers, 4-epicycloeucalenole and 4-epicyclomusalenone were isolated from fraction 10. 127

Figure 2-72. TLC plate of silica gel (left) and RP-18 (right) of fraction 3. The bands show the characteristic violet color 10of a triterpenoid on silica gel and blue color on RP-18. The peak contained 3.9 mg of 4-epicyloeucalenole and 4-epicyclomusalenone isomers elucidated by NMR spectroscopy (cf. 4.3.2). 128

Figure 2-73. ^{13}C NMR spectrum of the isomers 4-epicycloeucalenone and 4-epicyclomusalenone and the identification of side chain relevant double bonds and keto-functions (Above); HSQC and HMBC correlation in the cycloartenol-backbone of isomers 4-epicycloeucalenone and 4-epicyclomusalenone in fraction 10 from Baby Banana peel n-hexane extract fractionated by HSCCC (Below) (Oliveira et al. 2006; Akihisa et al. 1986; Knapp and Nicholas 1969a). 129

Figure 2-74. Relevant structure $^{2\text{-}3}J$-CH long–range correlation (HMBC) and (HSQC) in the side chains of 4-epi-cycloeucalenole (1A) and 4-epicyclomusalenone (1B, above). Cycloartenol-backbone (below, middle) and isomers of the 4-epi-cycloeucalenole (1A) and 4-epicyclomusalenone (1B, below) isolated from fraction 10 of a hexane extract from Baby Banana peels (Oliveira et al. 2006; Akihisa et al. 1986; Knapp and Nicholas 1969b). 131

Figure 2-75. APCI-MS spectra of 3-oxo-28-norcycloartane-type triterpenes with their 4-β-methyl-epimers which confirm the structure of 4-epi-cycloeucalenole and 4-epicyclomusalenone isolated in fraction 10 from a hexane extract of Baby Banana peels. 132

Figure 2-76. Schema of positive ion APCI-MS fragmentation of 3-oxo-28-norcycloartane-type triterpenes with their 4-β-methyl-epimers which confirm the structure of the 4-epi-cycloeucalenole and 4-epicyclomusalenone (Akihisa et al. 1997). 133

Figure 2-77. RP-18 TLC screening under white light and developed with anisaldehyde from the fractionation of HSCCC fraction 7 (15.4 g). The blue band in TLC showed that fraction 5 and 6 contained 2 mg of a pure compound which was submitted to 1/D and 2/D NMR experiments. 134

Figure 2-78. Chemical structure of ß-sitosterol according to HSQC, HMBC experiments (black arrows) and relevant COSY correlation both in the side chain and in the steroid skeleton of the structure (red arrows). 136

Figure 2-79. APCI spectrum (positive mode) of fraction 7 from HSCCC with ß-sitosterol at *m/z* 397.6 $[M\text{-}CH_3]^+$ together with an impurity of chlorophyll derivatives at *m/z* 874 at 21.4 min. 137

Figure 2-80. Schema of the characteristic fragmentation for Δ^5-sterols according to the APCI mass spectrum shown in Figure 2-79 (Kobayashi et al. 1993; Martinez 2002; Williams et al. 1963) 137

Figure 2-81. Schema of the characteristic pattern of fragments for Δ^5-sterols according to the mass spectrum shown in Figure 2-79 (Kobayashi et al. 1993 and Williams et al. 1963; Martinez 2002;Oliveira et al. 2006*)*. 138

Figure 2-82. First separation from Baby Banana peels by means of HSCCC with a solvent system Hexane/MeOH [2:1] in elution mode. Fractions 5 and 7 showed in elution mode the occurrence of chlorophyll derivatives. Pheophytin a was identified in fraction 7 by means of HPLC-APCI-MS-MS. 141

Figure 2-83. Second separation from Baby Banana peels by means of HSCCC with a solvent system ACN/MeOH [1:1] in elution and extrusion mode. Chlorophylls derivatives were identified by HPLC-APCI-MS-MS and TLC technique in fraction 1 of the extrusion mode. 142

Figure 2-84. APCI mass spectra of 1.5 mg of pheophytin *a* isolated by a preparative RP-18 –HPLC from fraction 1 (extrusion mode of HSCCC). The peak with a retention time of 22.1 min at *m/z* 872 $[M+H]^+$ corresponds to pheophytin *a* in concordance with literature data (Van Breemen et al. 1991a, 1991b; Hyvärinen and Hynninen 1999). 143

Figure 2-85. 600 MHz proton NMR spectrum of pheophytin *a,* 1.5 mg in CD_2Cl_2 purified from fraction 1 (extrusion mode of HSCCC separation) by means of preparative RP-18-HPLC (Smith et al. 1984). 144

Figure 2-86. Chemical structure of pheophytin *a* according to ^1H chemical shift reported in the literature (Smith et al. 1984). 146

Figure 2-87. HSCCC chromatograms of two separations of a methanol extract of Baby Banana peels using a solvent system of hexane/MeOH/water/EtOAc (10:10:1:1). Fractions 6 in the extrusion mode from both chromatograms were collected to isolate 3.3 mg of pheophytin *a*. 147

Figure 2-88. Chemical structure of pheophytin *a* isolated from Baby Banana peels (Lötjönen and Hynninen 1983). 149

Figure 2-89. ^{13}C NMR (above) and COSY spectra (below) of 3.3 mg of purified pheophytin *a* from Baby Banana peels in $CDCl_3$. The 2/D NMR spectra supported the ^{13}C chemical shift assignments depicted in Table 2-19. 151

Figure 2-90. Chlorophyll *a* and *b* bands identified by thin layer chromatography (silica gel) at white light and 366 UV from ethyl ether/hexane phase from spinach (solvent system: petroleum ether/ acetone/ dietylamine [10/4/1]) according to literature data (Minguez-Mosquera and Garrido-Fernández 1989). 156

Figure 2-91. Chromatogram of the HPLC-APCI-MS-MS of the ethyl ether/ hexane extract of spinach. Chlorophyll *a*, *b*, and pheophytin *a* eluted at 18.8 min, 21.1 min, and 23.7 min, respectively (Huang et al. 2008). 156

Figure 2-92. APCI-HPLC-MS-MS data of chlorophyll *a* from spinach ethyl ether/ hexane extract with *m/z* 893.5. Chl-*a* is the major peak in the extract (Huang et al. 2008). 157

Figure 2-93. APCI-HPLC-MS-MS data of chlorophyll *b* from spinach ethyl ether/ hexane extract with *m/z* 908.1. Chl-*b* is the minor peak in the extract (Huang et al. 2008). 157

Figure 2-94. APCI-HPLC-MS-MS data of pheophytin *a* from spinach ethyl ether/ hexane extract with *m/z* 872.1 (Huang et al. 2008). 158

Figure 2-95. Analysis of the solvent system Hex/MeOH [1:1] by thin layer chromatography (TLC) to evaluate the partition coefficient qualitatively through the distribution in the lower and upper phase.

The plate shows if the solvent system is suitable to separate triterpenoids present in the mixture which are represented as bands in the lower phase (L_{ph}) and upper phase (U_{ph}). 162

Figure 2-96. The analysis of a hexane /EtOH/ water [6:5:2] solvent system to optimize the isolation of chlorophylls and their derivatives in grass by HSCCC by application of thin layer chromatography for qualitative evaluation of the partition coefficient in lower (L ph) and upper phases (U ph). 163

Figure 2-97 Spinach extracts of diethyl ether/hexane with chlorophylls and xanthophylls (left) and of the hexane phase with carotenoids (right). 167

Figure 2-98. HSCCC chromatogram of a separation of 486 mg of ethyl/hexane extract from spinach. Eight fractions in elution mode and fifteen in extrusion mode were obtained. Xanthophylls and chlorophylls were identified by APCI-HPLC-MS-MS and isolated by HSCCC. 168

Figure 2-99. Elution fractions of xanthophylls in spinach identified by APCI-HPLC-MS-MS. Fraction 7 was not clearly identified. Neoxanthin (F4), canthaxanthin (F5), neochrome/ luteoxanthin (F6) and lutein (F8). 168

Figure 2-100. The characteristic color of chlorophyll *a* was observed during the extrusion mode for first time in the spinach HSCCC separation and recorded during the recollection of the fractions. 170

Figure 2-101. APCI-HPLC-MS-MS spectrum of chlorophyll *a* in fraction 13 with a quasimolecular ion of *m/z* 894 $[M+H]^+$ at 20.9 min (Huang et al. 2008; Van Breemen et al. 1991b). 170

Figure 2-102. The characteristic color of chlorophyll *b* was observed during the extrusion mode for first time in the spinach HSCCC separation and was recorded during the recollection of the fractions. 171

Figure 2-103. APCI-HPLC-MS-MS spectrum of chlorophyll *b* in fraction 6 with a the quasimolecular ion of *m/z* 907 $[M+H]^+$ at 18.4 min (Huang et al. 2008; van Breemen et al. 1991b). 171

Figure 2-104. ^{13}C NMR in spectra of chlorophyll *b* isolated from spinach by HSCCC recorded at 150 MHz in $CDCl_3$. 172

Figure 2-105. ^{1}H NMR spectra of chlorophyll *b* isolated from spinach by HSCCC recorded at 600 MHz in $CDCl_3$. 172

Figure 2-106. Structure and numbering of chlorophyll *a* (C-3_a = CH_3) and *b* used throughout this section (Abraham and Rowan 1991). 174

Figure 2-107. ^{13}C NMR spectra of chlorophyll *a* isolated from spinach by HSCCC recorded at 150 MHz in CD_2Cl_2 176

Figure 2-108. ^{1}H NMR spectra of chlorophyll *a* isolated from spinach by HSCCC recorded at 600 MHz in CD_2Cl_2. 176

Figure 2-109. HSCCC chromatogram (grass extract) with elution and extrusion mode. Solvent system: hexane-dichloromethane-ethanol-water (4/2/6/2). Chlorophyll separation showed a higher resolution in comparison to xanthophylls in elution and extrusion mode. 179

Figure 2-110. HSCCC chromatogram (grass extract) with elution and extrusion mode. Solvent system: hexane-chloroform-ethanol-water (4/2/6/2). Xanthophyll separation showed a higher resolution in elution mode in comparison to the chlorophyll separation in extrusion mode. 180

Figure 2-111. HSCCC chromatogram of chlorophylls and derivatives from grass extract using hexane/EtOH/CH_2Cl_2/H_2O [6:2:4:2] as solvent system. 186

Figure 2-112. HSCCC chromatogram of chlorophylls from spinach extract by using hexane/EtOH/$CHCl_3$/H_2O [6:2:4:2] as solvent system. 186

Figure 2-113. HSCCC chromatogram of chlorophylls and their derivatives from Baby Banana control peel extract using the solvent system hexane/EtOH/CH_2Cl_2/H_2O [6:2:4:2]. 188

Figure 2-114. HSCCC chromatogram of chlorophylls and their derivatives from Baby Banana peel extract with hyperpigmentation using the solvent system hexane/EtOH/CH_2Cl_2/H_2O [6:2:4:2]. 188

Figure 2-115. The chlorophyll cycle of higher plants, whereby Chl *a* and *b* are interconverted via 7-hydroxy Chl-*a* (Hörtensteiner 1999; Vicentini et al. 1995). 189

Figure 2-116. 34.92 kg of hyperpigmented Baby Banana produced 401.6 g freeze-dried peels that were analyzed by Spiral-Coil-LSRCCC. 190

Figure 2-117. Spiral-Coil Assembly of the CCC prototype that combines two advantages in comparison with the Low Speed Rotary Countercurrent chromatography such as short separation time and large sample load. It is a preparative model for semi-industrial scale separations. 191

Figure 2-118. Spiral-Coil LSRCCC chromatogram of 10 g of a hexane extract from Baby Banana peels with hyperpigmentation (HP) in elution and extrusion mode. 193

Figure 2-119. Spiral-Coil LSRCCC chromatogram of 17 g from Baby Banana peels with hyperpigmentation (HP). The fractions were identified by means of APCI-HPLC-MS-MS as chlorophylls derivatives (red color). The green bands depict the chlorophyll derivatives linked to sterols. The mass spectra of the fractions were compared with literature data (Huang et al. 2008; Eckardt et al. 1991; van Breemen 1991ab). 195

Figure 2-120. Nomenclature of chlorophylls and their derivatives (Huang et al. 2008; Katz et al. 1968). 196

Figure 2-121. Fraction 1 of elution mode corresponds to 19.9 mg of 1,2 diacyl-phosphorylcholine and fraction 3 to 154.7 mg of lutein in Spiral-Coil-LSRCCC chromatogram (Left), which were identified by comparison with authentic standards isolated by HSCCC. Tubes of Spiral-Coil-LSRCCC of 154.7 mg of lutein in elution mode identified by APCI -HPLC-MS-MS (Right). 204

Figure 2-122. Positive-ion APCI HPLC-MS-MS spectrum of 1,2 diacyl-phosphorylcholine in fraction 1 from elution mode obtained by Spiral-Coil-LSRCCC from Baby Banana peels with hyperpigmentation. 205

Figure 2-123. Positive-ion APCI HPLC-MS-MS spectrum of lutein (*m/z* 551.4) in fraction 3 of elution mode from Spiral-Coil-LSRCCC (Yuan et al. 1997). 206